


Article

Investigation of the Formation Mechanism and Environmental Risk of Tire—Pavement Wearing Waste (TPWW)

Kechen Wang ¹, Xiangyu Chu ², Jiao Lin ², Qilin Yang ², Zepeng Fan ^{3,*}, Dawei Wang ^{2,3,*}  and Markus Oeser ³

¹ School of Information Engineering, Harbin University, Harbin 150086, China; w.kc@163.com

² School of Transportation Science and Engineering, Harbin Institute of Technology, Harbin 150090, China; xychu@hit.edu.cn (X.C.); jiaolin@hit.edu.cn (J.L.); yangqilin@stu.hit.edu.cn (Q.Y.)

³ Institute of Highway Engineering, RWTH Aachen University, 52074 Aachen, Germany; oeser@isac.rwth-aachen.de

* Correspondence: fan@isac.rwth-aachen.de (Z.F.); wang@isac.rwth-aachen.de (D.W.)

Abstract: Tire—pavement interaction behaviours result in large amounts of wearing waste matter, which attaches to the surface of the pavement and is directly exposed to the surrounding environment. This kind of matter imposes a great challenge to the environment of the road area. The current study is devoted to carrying out a comprehensive investigation of the formation mechanism of tire—pavement wearing waste (TPWW), as well as the resulting environmental risks. A self-developed piece of accelerated polishing equipment, the Harbin advanced polishing machine (HAPM), was employed to simulate the wearing process between vehicle tires and pavement surfaces, and the TPWW was collected to conduct morphological, physical, and chemical characterisations. The results from this study show that the production rate of TPWW decreases with the increase in polishing duration, and the coarse particles (diameters greater than 0.425 mm) account for most of the TPWW obtained. The fine fraction (diameter smaller than 0.425 mm) of the TPWW comprises variously sized and irregularly shaped rubber particles from the tire, as well as uniformly sized and angular fine aggregates. The environmental analysis results show that volatile alkanes (C9–C16) are the major organic contaminants in TPWW. The Open-Graded Friction Course (OGFC) asphalt mixture containing crumb rubber as a modifier showed the highest risk of heavy metal pollution, and special concern must be given to tire materials for the purpose of improving the environmental conditions of road areas. The use of polyurethane as a binder material in the production of pavement mixtures has an environmental benefit in terms of pollution from both organic contaminants and heavy metals.

Keywords: asphalt pavement; wearing waste; environmental risk; heavy metal; organic contaminant



Citation: Wang, K.; Chu, X.; Lin, J.; Yang, Q.; Fan, Z.; Wang, D.; Oeser, M. Investigation of the Formation Mechanism and Environmental Risk of Tire—Pavement Wearing Waste (TPWW). *Sustainability* **2021**, *13*, 8172. <https://doi.org/10.3390/su13158172>

Academic Editors: Andrew Shing-Tao Chang and Chaohui Wang

Received: 16 June 2021

Accepted: 16 July 2021

Published: 21 July 2021

Publisher's Note: MDPI stays neutral with regard to jurisdictional claims in published maps and institutional affiliations.



Copyright: © 2021 by the authors. Licensee MDPI, Basel, Switzerland. This article is an open access article distributed under the terms and conditions of the Creative Commons Attribution (CC BY) license (<https://creativecommons.org/licenses/by/4.0/>).

1. Introduction

In the service life of pavement, due to the wearing interactions between vehicle tires and pavement surfaces, the wearing of vehicles' mechanical parts, the deposition of vehicles' gas emissions and atmospheric dust, and other reasons, pollutant particles accumulate on pavement surfaces. Among all of these potential sources, the wearing waste particles from the interaction of vehicle tires and pavement surfaces are the main contributors to the quantity of pollutants. TPWW is mechanically generated by the rolling shear of a tire against a pavement surface, and it comprises tire wear, road wear, and brake wear [1,2]. The pavement surface runoff carries a great number of these pollutants and flows through the surrounding soil and water bodies, which causes the accumulation, transmission, and migration of the pollutants in the road area. Unlike the point source pollution from industrial wastewater and urban sewage, which can be uniformly collected and centrally treated, road area pollution is a scattered, sparse plane network system, which greatly increases the difficulty of controlling the pollution.

The formation mechanism and environmental risks of TPWW are matters of general concern. Day et al. first introduced the concept of “urban street dust” to investigate the

importance of dust as a component of the lead intake of urban children [3]. Since then, more research attention was given to the relationship between pavement surface dust and runoff pollution [4–7]. It is well recognised that pavement TPWW, which includes tire wear particles, asphalt mixture wear particles, and road-marking wear particles, is the main source of pavement surface runoff pollution—suspended solids (SSs). The tire material is the main source of Zn, Fe, Cd, Cu, Pb, and other heavy metals in SSs, while the road material contributes the main organic solids, such as polycyclic aromatic hydrocarbons and phenols. The main components of tires are rubber, carbon black, metal, fabric, and various additives (such as plasticiser, sulphur, anti-aging agent, zinc oxide, etc.). Among them, the rubber composition accounts for about 45–48% of the tire mass, carbon black accounts for about 22%, metals account for about 15–25%, and auxiliaries account for about 10% [8,9]. Hong et al. used a quantitative method for measuring the contribution of tires to road surface pollutants in road sediments [10]. In addition, Tian et al. found that *N*-(1,3-dimethylbutyl)-*N'*-phenyl-*p*-phenylenediamine (6PPD), a globally ubiquitous tire rubber antioxidant that is widely used in tire additives, would produce highly toxic 6PPD–quinone during tire production and use, which was the main cause of the death of salmon in roadside waters [11].

The chemical composition of asphalt is extremely complex, and the most important elements are carbon and hydrogen. In addition, there are small amounts of oxygen, nitrogen, and sulphur, which are often referred to as heteroatoms. In the production of natural asphalt, it has been found that there are more than 50 kinds of trace elements, which are mainly Fe, Ni, V, Al, Na, Ca, Cu, Cl, Br, and I; generally, the V, Ni, and Fe contents are the greatest. Generally, different organic solvents or different adsorbents are used to selectively dissolve asphalt into several components with similar chemical properties and a colloidal structure. The four components of asphalt are asphaltene, resin, aromatic, and saturate [12]. Viana et al. [13] measured the content of chromium and nickel in petroleum asphalt, and Souza et al. carried out a spectral analysis of vanadium in asphalt [14]. Sugiyama proposed an ICP–MS-based heavy metal detection method [15]. Gab–Allah et al. [16] summarised and analysed the methods of analysis of sulphur and heavy metal elements in petroleum products. Niles et al. studied the influence of sunlight on pollutant precipitation by using a simulated illumination method, and the results showed that the amount of precipitation of organic matter in water during one week of sunlight irradiation was more than 25 times that in a dark environment [17]. Brandt extracted and measured PAHs in asphalt by using a dynamic leaching experiment [18]. Road-marking materials generally consist of fillers, auxiliaries, and solvents, which may contain volatile organic compounds, benzene series, halogenated hydrocarbons, alcohols, esters, ketones, and soluble heavy metals [19]. Jin et al. found lead, cadmium, mercury, chromium, and other heavy metals in paint by means of microwave digestion and inductively coupled plasma emission spectrometry. In addition, the national standard GB/T 36488–2018 specifies the use of gas chromatography–mass spectrometry for the determination of polycyclic aromatic hydrocarbons in coatings [20]. Pan et al. analysed the migration amounts of PAHs in paint by using solid-phase microextraction/gas chromatography–mass spectrometry [21].

Despite the numerous studies regarding the chemical characteristics of pavement and tire materials, little knowledge has been established on the formation of TPWW or its potential environmental risks in road areas. The current study was motivated by this. In this study, an accelerated polishing equipment, namely the Harbin Advanced Polishing Machine (HAPM), was developed, and the wearing process of vehicle tire and pavement surface materials was simulated in the laboratory. The wearing waste matters were collected, and the morphological and chemical properties of the obtained waste as well as their environmental influences were identified. The findings from the current study provide guidance for the design of environmentally friendly asphalt pavement and the improvement of road area ecological environment.

2. Materials and Methods

2.1. Raw Materials

Three kinds of binders were used in this study, including virgin asphalt, crumb rubber modified asphalt, and polyurethane. The asphalt with a penetration grade of 60/80 (Pen 70), from Sinopec Zhenhai Refining and Chemical Co., Ltd. (Ningbo, China) was used as the virgin asphalt. The crumb rubber modified asphalt was produced from the same asphalt. The polyurethane with an isocyanates–polyhydric alcohol ratio of 800:100 was obtained from BASF SE (Shanghai, China) [22–24]. The limestone and andesite were used as filler and aggregate, respectively.

Two types of pavement mixtures, AC-13 and OGFC-13, were selected as the research objects. The AC-13 and OGFC-13 are two commonly used asphalt mixtures in the surface course of asphalt pavement. The AC-13 asphalt mixture contains dense-graded aggregates, and it is of the void content of 3~6%. The OGFC-13 asphalt mixture comprises open-graded aggregates, and the void content of OGFC-13 is generally greater than 18%. Due to the differences in the microstructure of AC-13 and OGFC-13, the technical requirements on the binder materials of the two mixtures are significantly different. The virgin bitumen with the penetration grade of 70 is the most used binder material in AC-13, whereas the modified bitumen binders with higher viscosity are generally used in OGFC-13 to improve the ravelling resistance. The polyurethane has been recently introduced into the construction of permeable pavement and was therefore only used to fabricate the OGFC-13 mixture. The aggregate grading curve of AC-13 and OGFC-13 are shown in Figure 1. The asphalt mixtures were made into plates with a length, width, and height of 300 mm, 300 mm, and 50 mm, respectively, the same as the rutting test samples. The fabricated test specimens are shown in Figure 2. Table 1 presents the types and compositions of all specimens.

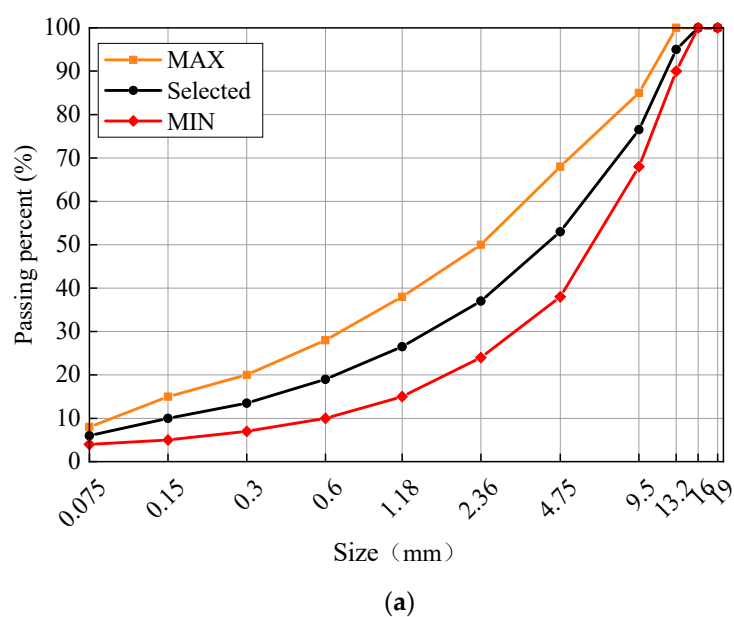


Figure 1. Cont.

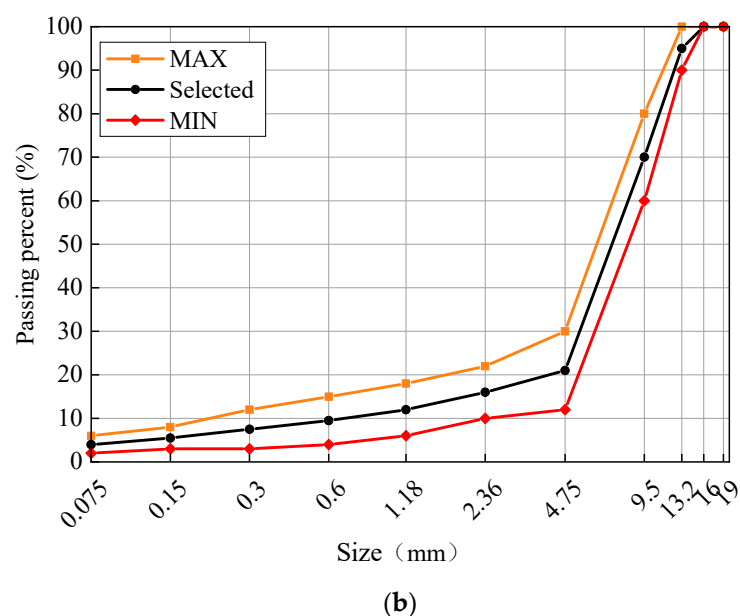


Figure 1. Gradation curves of (a) AC-13 and (b) OGFC-13.



Figure 2. The fabricated samples used for the polishing test.

Table 1. The composition of samples.

Sample Number	Grading	Aggregate and Filler	Binder	Binder Content
Group I	AC-13	Andesite and limestone	Virgin asphalt	5.0%
Group II	OGFC-13		Rubber modified asphalt	4.6%
Group III	OGFC-13		Polyurethane	4.6%

2.2. Wearing Test

The wearing tests were conducted by the Harbin Advanced Polishing Machine (HAPM), as shown in Figure 3. The HAPM contains six units: an acceleration system, loading system, workbench system, dispenser system, protection system and operation control system. The acceleration system was used to set the loading rate and provide power for the tests. The radial tire (185/60 R 14, produced by Giti Company) was used for the HAPM test in the current study. The section width, aspect ratio and hub diameter of the tire are 185 mm, 60, and 14 inches, respectively.



Figure 3. The self-developed Harbin Advanced Polishing Machine (HAPM).

During the test, the specimen was fixed in the slot of the workbench, and the surface of the specimen was flush with the workbench. The silica sand was selected as the polishing medium, since previous research has demonstrated that the silica sand can best simulate the effect of pavement dust. A total of 50 g of silica sand was uniformly distributed on the specimen surface through the dispenser system. The water was continuously sprayed at the rate of 60 mL/min through the sprinkler in the dispenser system during the loading process to cool the wearing system and reduce the wearing noise. The contact pressure between the tire and sample surface was set as 1500 N, and the rotation rate of the tire was set as 100 rad/min. The major parameters for the wearing test are given in Table 2. The determination of the parameter values was based on our previous research in combination with a trial-and-error test [25–27]. Each wear test cycle was 30 min, and 5 cycles were carried out for every specimen. The wearing products were collected for subsequent analysis after every cycle test.

Table 2. The parameters of wear test.

Parameter	Rotation Rate	Contact Pressure	Polishing Media	Sprinkling Rate	Temperature
Value	100 rad/min	1500 N	50 g silica sand	60 mL/min	20 °C

2.3. Physical Analysis of TPWW

For purpose of analysing the physical characteristics of the TPWW, the vacuum freeze-drying method was employed for the solid–liquid separation of the original wearing products. After that, the volumes of the TPWW matters were measured, and the particle size distributions of the TPWW were determined through the sieve test. The morphological properties of the fine TPWW particles (size smaller than 425 μm) were also characterized with the help of the Scanning Electron Microscope (SEM) test.

2.4. Chemical Analysis of TPWW

2.4.1. Heavy Metals Analysis

In a spectroscopic elemental analysis sample preparation, acid digestion is an important step of the entire analytical procedure. In this research, HNO_3 , HClO_4 and HCl were used for acid digestion. Samples were accurately weighed (0.1 g each) and placed in a 150 mL conical flask. Then, 2.5 mL of HNO_3 and 7.5 mL of HCl were mixed and poured into a conical flask slowly. Then, the mixture was boiled gently for about 30 min. After cooling, 3 mL of HClO_4 was added, and the mixture was gently boiled until dense white

fumes appeared. Later, the mixture was allowed to cool, and 5 mL of deionized water was added, followed by further boiling until the fumes were totally released. Afterwards, 5 mL of 10% HCl was added, and the mixture was gently boiled for about 10 min. During the digestion procedures, the inner walls of the flasks were washed with 2 mL of 2% HNO₃ to prevent the loss of the samples, and at the last part of the digestion processes, the samples were filtered with filter paper. Then, a sufficient amount of HNO₃ was added to make the final volume up to 50 mL.

The content of heavy metal elements in raw pavement materials and wear products was determined by inductively coupled plasma atomic emission spectrometry (ICP-AES). The samples were aspirated in the atomizer by the nebulizer to measure the analyte concentration. The plasma flow rate, auxiliary gas flow rate, atomizer flow rate and injection flow rate were set as 15 L/min, 0.2 L/min, 0.8 L/min, 1.5 mL/min, respectively. The standard soil sample was used as the control sample. In this research, Cd, Pb, Cr, Cu, and Zn were target elements to be measured. The concentration (C) of the target element in the sample was calculated by Equation (1) as follows:

$$C = \frac{C_i \times V}{m} \quad (1)$$

where C is the concentration of the target element in the sample, mg/kg; C_i is the measured concentration of the target element in the sample, µg/mL; V is the metered volume of the sample, mL; m is the mass of the sample, g.

2.4.2. Organic Pollutants Analysis

The gas chromatography–mass spectrometry (GC-MS) method was used to determine the composition of organic compounds in wear products. An ultrasonic extraction pre-treatment was needed for the collection of the TPWW products before the GC-MS test. About 2~3 g of the sample was mixed with anhydrous sodium sulphate to remove all moisture. Then, 40 mL of n-hexane was added, and the mixture was treated by ultrasonic extraction for 30 min. Later, the sample was filtered with a filter paper with 0.45 µm particle retention. The filtrate was used for measuring the chromatogram and target ion abundance of the sample in the GC-MS test. A schematic flowchart of the experimental test in this study is shown in Figure 4.

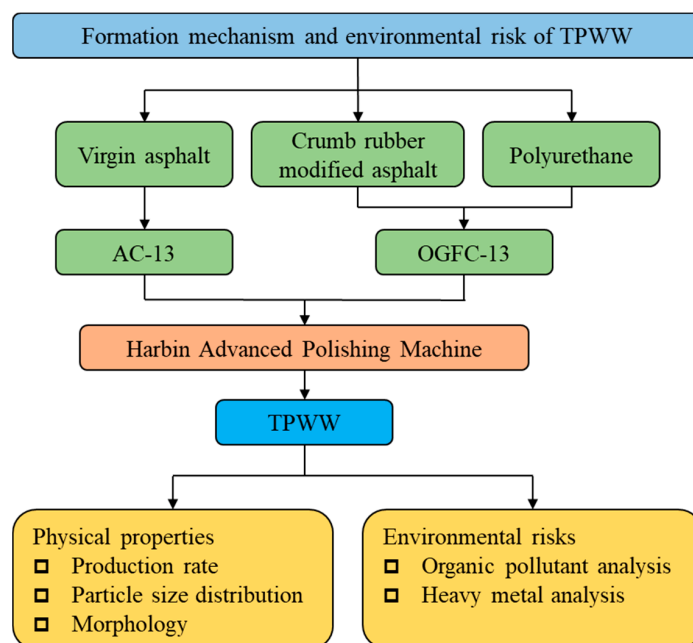


Figure 4. Schematic flowchart of the current study.

3. Results and Discussion

3.1. Formulation of TPWW

The measured volumes of the TPWW after every 30 min of polishing duration are shown in Figure 5. It can be easily found that the amount of TPWW generally decreases as the polishing procedure continues. The exception is that of group I at the end of the 120 min polishing duration. The slight increase in the TPWW at the end of the 120 min polishing duration was found to be resulted from the stripping of aggregates by observation. The results from Figure 5b indicate that the polishing resistance of the polyurethane (PU) mixtures is better than that of the bituminous mixtures, and the polishing resistance of the AC-13 asphalt mixture is better than the OGFC-13 asphalt mixture.

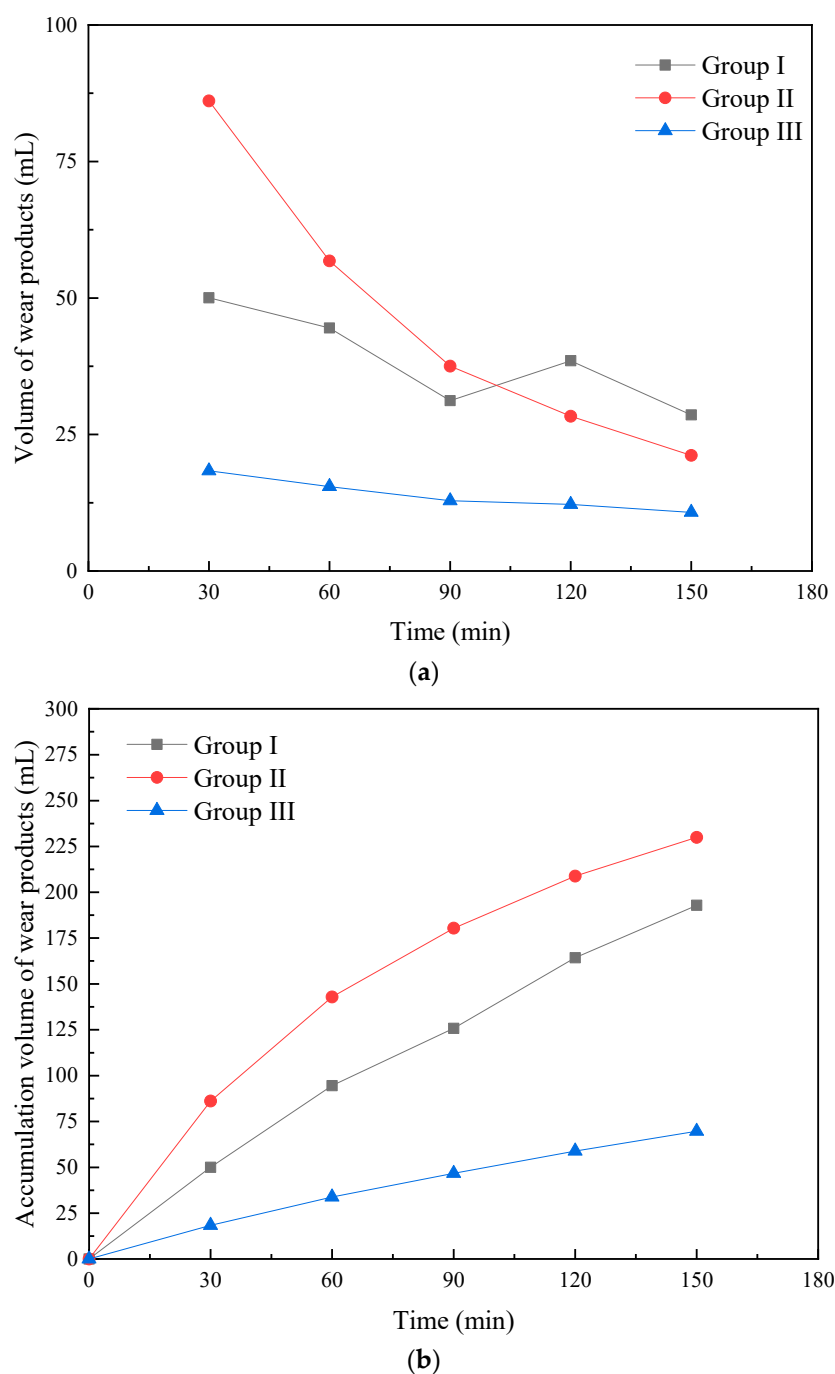


Figure 5. The (a) production rate and (b) accumulation of TPWW during the test.

3.2. Particle Size Distribution of TPWW

The wearing products directly collected from the HAPM test contain a certain amount of particles whose sizes are greater than 1.7 mm. However, this fraction of TPWW was eliminated during the following analysis due to the following reasons: (i) this fraction of particle is the mineral aggregates directly stripped from the test sample surface, and they are very different from the wearing products in terms of formation mechanism; (ii) these particles are of higher volume and mass values than that of the finer particles, and they will hold a dominant position in both volume and mass of the total wearing products if they are taken into consideration. However, these particles hardly contribute to the organic contaminant and heavy metal elements of the road area environment. The remaining fraction (size smaller than 1.7 mm) constitutes both aggregate and rubber wearing particles. They were divided into five groups which were of the particle size range of 0~0.105 mm, 0.105~0.25 mm, 0.25~0.425 mm, 0.425~0.85 mm, and 0.85~1.7 mm, respectively. The identified particle size distributions of different groups of TPWW are shown in Figure 6. It is found from Figure 6 that the coarse particles (0.425~1.7 mm) dominate the TPWW regardless of the asphalt mixture type, which accounts for nearly 90% of the total collections. Among the three sample groups, group I is of the least content of coarse particles which can be attributed to the denser microstructure of the AC-13 asphalt mixture.

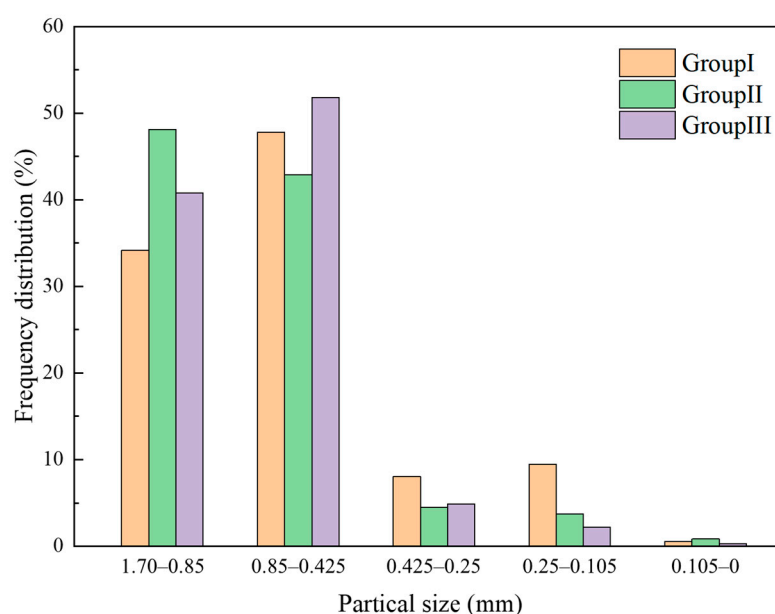


Figure 6. The particle size distribution of the TPWW.

3.3. Morphology of TPWW

The morphology of the fine particles (smaller than 0.425 mm) was characterized through SEM, and the results are shown in Figures 7 and 8. The selection of the fine particles was based on the fact that the TPWW of a diameter smaller than 500 μm can be well dissolved in water media, as has been demonstrated in previous research [28]. The mesoscale morphologies (see Figure 7) of the TPWW indicate that the finalized materials were composed of varying-sized and irregular-shaped rubber particles from the tire, as well as uniform-sized and angular fine aggregates. The microscale morphologies (found in Figure 8) of the fine aggregates and rubber particles exhibit significantly different features. The rubber particles were obviously porous, with a great number of fine fillers adsorbed on the surface. The aggregation phenomenon of the fine fillers can also be observed in certain regions. On the other hand, the aggregate particles had relatively smooth surfaces and profound angularity.

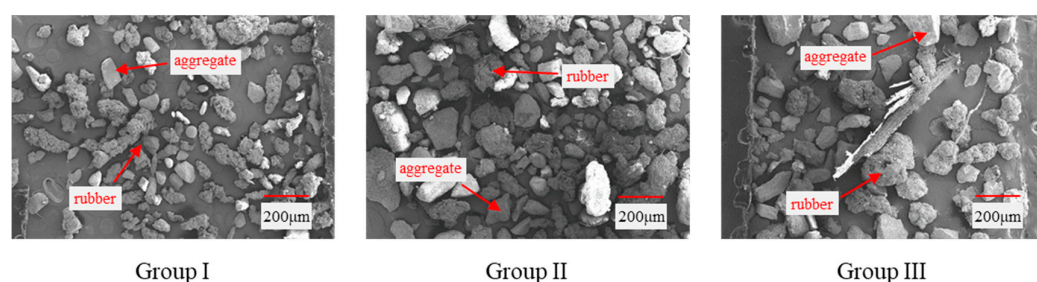


Figure 7. Mesoscale morphology of the TPWW.

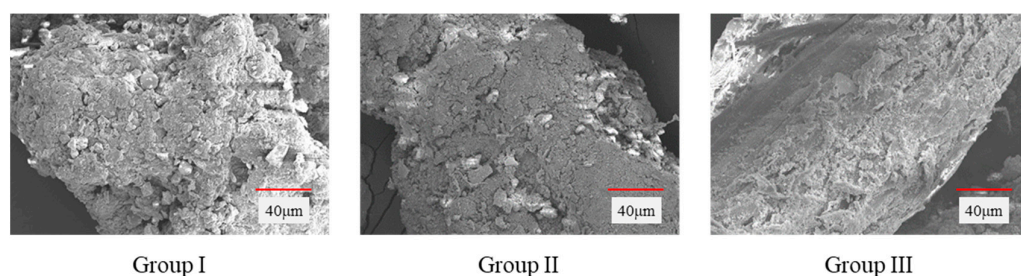


Figure 8. Microscale morphology of the TPWW.

3.4. Environmental Analysis of TPWW

3.4.1. Organic Contaminant Content of TPWW

The measured results of the gas chromatography test for the three groups of samples are presented in Figures 9–11, respectively. The mass content of each component was determined by the gas chromatography area, and the calculation results are shown in Figure 12. It is seen that the alkanes account for nearly 80% of the total TPWW matters, followed by the haloalkanes (8~10%). The benzene series with stronger toxicity shows a relatively low content of no more than 5%. The contents of alkenes for the three groups are generally no more than 1%. The remaining matter includes some esters, ethers, alcohols, etc. The group II sample is found to contain more benzene series substances compared to the group I sample. The increased benzene series substances are introduced by the use of crumb rubber modifiers. The substitution of polyurethane as the binding material leads to a decrease in the content of alkanes as well as an increase in benzene series substances. The group III sample shows the highest content of remaining substances (7.54%). This is resulted from the increased esters and aldehydes (including methyl stearate, petroselinic acid methyl ester, benzaldehyde, etc.) which are the by-products of polyurethane.

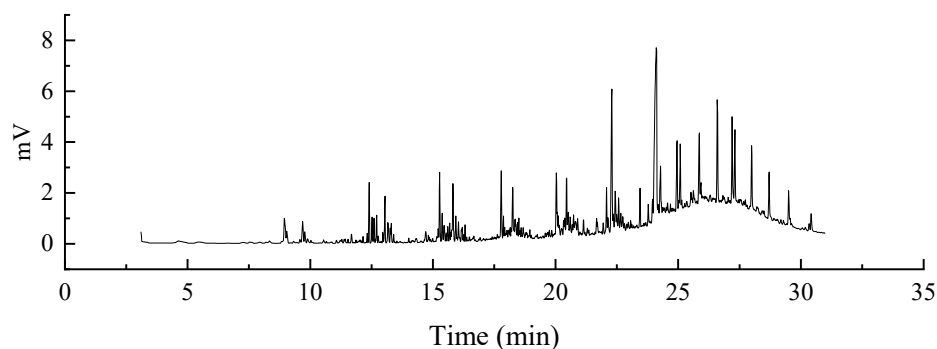


Figure 9. Chromatogram of the group I sample.

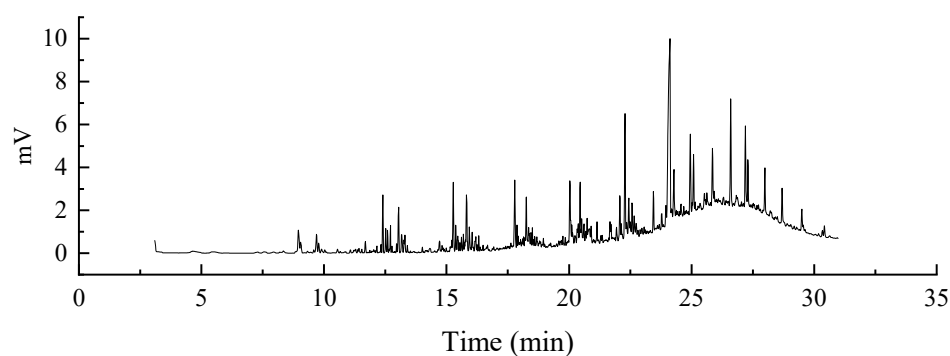


Figure 10. Chromatogram of the group II sample.

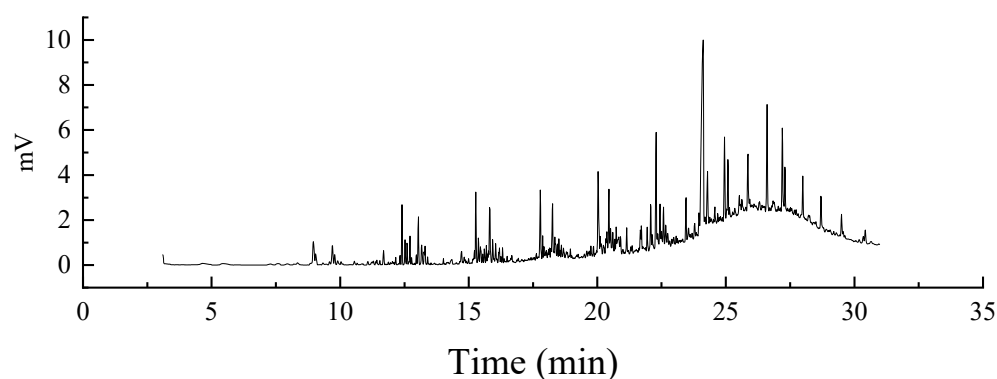


Figure 11. Chromatogram of the group III sample.

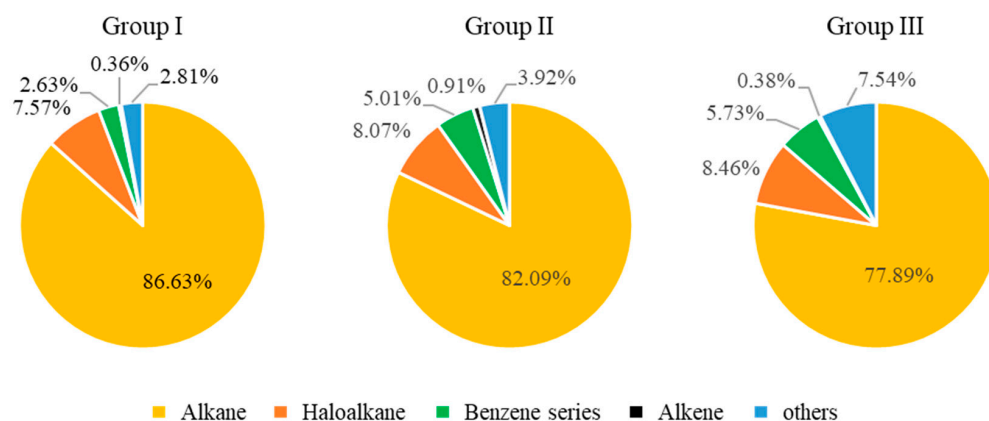


Figure 12. Percentages of the various organic matters in different groups of samples.

The separated components in the gas chromatography analysis were further characterized by the mass spectrometry method. By comparing the obtained results to the standard mass spectra information in the NIST.17 database, the major compositions of the TPWW matters were identified as shown in Table 3. It shows that the alkanes are of ~75% of the total detectable substance types, followed by the benzene series with an approximate content of 15%. The haloalkanes, alkenes, and others (esters, ethers, alcohols, etc.) make up ~10% of the content. Among the alkanes, the volatile C9–C16 alkanes account for nearly half of the detected substances. The boiling point of alkane increases with the carbon number and carbon chain, and the alkanes with a carbon number of 9 generally have a boiling point of nearly 150 °C. This is reasonable considering that the mixing temperature of asphalt mixture is normally in the range of 140–150 °C. The alkanes whose carbon numbers are smaller than 9 can be readily volatilized during the mixing procedure, and

therefore, they hardly exist in the TPWW. The benzene series substances mainly include methylbenzene, naphthalene, anthracene, phenol, and their derivatives.

Table 3. Quantities of different detected matters.

	Alkane	Haloalkane	Benzene Series	Alkene	Others	Sum
Group I	53	2	12	1	4	72
Group II	58	4	11	2	4	79
Group III	53	5	10	1	4	73

To summarize, the organic contaminant characteristic of TPWW is closely related to the binder materials, the mixing conditions, the chemical composition of the tire, and the pavement surface properties. From the aspect of pavement materials, the virgin asphalt resulted TPWW shows low toxicity, and the addition of asphalt modifiers can cause increased toxicity. A higher mixing temperature can increase the loss of the volatile fractions in the asphalt binder, which in turn decreases the volatility of the TPWW. Comparing to the asphaltic mixtures, the use of polyurethane shows additional environmental benefits [29–31].

3.4.2. Heavy Metal Content of TPWW

The measured heavy metal contents of the virgin asphalt binder, modified asphalt binder, tire particles, and the collected TPWW materials (particle size smaller than 0.425 mm) are presented in Table 4.

Table 4. Contents of the heavy metals in the various materials (mg/kg).

	Cd	Pb	Cr	Cu	Zn
Virgin asphalt	0.23	5.64	14.45	9.03	36.23
Modified asphalt	0.25	5.25	20.76	8.23	125.06
Vehicle tire	0.20	12.42	54.44	7.44	1458.08
Group I	0.69	13.93	545.27	25.87	1513.90
Group II	2.18	21.46	638.95	38.40	2192.22
Group III	0.54	15.32	218.16	14.43	1251.21

Results from Table 4 show that the virgin asphalt binder contains relatively low heavy metal among the four raw materials. The contents of Pb, Cr, and Zn elements in the tire particles were approximately 2, 4, and 40 times higher than that of the virgin asphalt binder, respectively. The higher contents of Cr and Zn heavy metals in the modified asphalt compared to the virgin asphalt are expected to be sourced from the crumb rubber modifier. It is also found from Table 4 that the collected TPWW from group II samples has the highest contents of all the five detected heavy metals. The higher contents of heavy metals for the group II TPWW matters can be resulted from both the use of crumb rubber modifier and the greater amount of accumulated TPWW. Even though that the asphalt pavement composed of the OGFC-13 mixture has the advantage of higher skid resistance and noise reduction, the associated environmental risks must be considered. In general, the group III samples have the lowest content of the five heavy metal elements, which implies a potential environmental benefit of using polyurethane for the replacement of asphalt binder materials.

The TPWW is the major component of the pavement surface dust and pavement water contaminants. For the purpose of comparison, the current study collected the reported data of the heavy metal element content of the pavement surface dust in several cities (see Table 5). Detailed information regarding the location as well as the heavy metal contents are given in Table 3. It is found that the contents of the Cd element in the TPWW matters are generally higher than that of the measured pavement surface dust, especially for the group II samples with modified asphalt binder. The contents of the Pb element in groups I, II, and III are lower than that of the reported data from different cities. However, the

measured values of Cr and Zn content in pavement surface dust are found to be lower than that of the TPWW matters which indicating an enrichment effect of the Cr and Zn elements in the wearing process. On the other hand, the Cu contents in pavement surface dust are slightly higher than that of the lab-obtained samples.

Table 5. Contents of heavy metals in the urban street surface of different cities.

City	Cd	Pb	Cr	Cu	Zn
Villavicencio [32]	–	87.5	9.4	126.3	133.3
Black Sea coast [33]	0.4	59	59	132	457
Bandar Abbas [34]	0.42	60	74	149	293
Kuala Lumpur [35]	0.23	43.53	36.05	116.39	89.22
Massachusetts [36]	–	73	95	105	240
Beijing [37]	0.34	70.79	87.59	70.26	250.54
Xi'an [38]	–	124.5	145.0	54.7	268.6
Nanchang [39]	0.58	62	–	102	208
Korla [40]	0.06	37.93	56.44	34.33	–
Shenzhen [41]	0.67	136.46	75.86	108.97	286.57

4. Conclusions

This study contributes to a comprehensive understanding of the TPWW by conducting a variety of polishing tests and materials characterization. The major conclusions from this study include:

The production rate of TPWW decreases with the increasing polishing duration, and the coarse fraction (diameter greater than 0.425 mm) accounts for nearly 90% of the total TPWW. Among the fine TPWW matters, the rubber particles are of a porous microstructure with fine fillers adsorbed on the surface, while the aggregate particles had a relatively smooth surface and profound angularity.

Alkanes are the main source of organic contaminants in the TPWW matters, with an average percentage of 80%, and half of the detectable alkanes are volatile C9–C16 substances. The toxic benzene series substances show a relatively low content which is no more than 5%. The tire is found to be closely related to the heavy metal pollution in the road area, and the potential environmental risks arising from the use of crumb rubber modifier and OGFC asphalt mixture must be carefully treated.

The findings from the current study provide insights into the formation mechanism and environmental risk of the tire–pavement TPWW matters. However, the mode of occurrences of the detected heavy metal elements remains unclear, and the bioavailability of heavy metals is not involved. Besides, pollutant transportation is not involved in the current study, and should be further identified in future research.

Author Contributions: Conceptualization, Z.F.; Investigation, K.W. and X.C.; Methodology, Z.F.; Supervision, D.W.; Validation, Q.Y., Z.F. and M.O.; Writing—Original Draft, K.W., X.C. and J.L. All authors have read and agreed to the published version of the manuscript.

Funding: This research was funded by the Education Department of Heilongjiang Province, grant number SJGZ 20190035; German Research Foundation (DFG), grant number OE 514/15–1 (459436571).

Institutional Review Board Statement: Not applicable.

Informed Consent Statement: Not applicable.

Data Availability Statement: The data presented in this study are available on request from the corresponding author. The data are not publicly available due to confidentiality promised to research participants.

Acknowledgments: The authors would like to thank all reviewers for their valuable comments on this thesis, which allowed us to find many details worthy of improvement and made our paper more clear and complete.

Conflicts of Interest: The authors declare no conflict of interest.

References

1. Yang, G.; Wang, H.; Pan, Y. Detection and evaluation methods of pavement wearing based on multi-line texture. *China J. Highw. Transp.* **2016**, *29*, 35–40.
2. Wagner, S.; Hüffer, T.; Klöckner, P.; Wehrhahn, M.; Hofmann, T.; Reemtsma, T. Tire wear particles in the aquatic environment—a review on generation, analysis, occurrence, fate and effects. *Water Res.* **2018**, *139*, 83–100. [[CrossRef](#)] [[PubMed](#)]
3. Day, J.P.; Hart, M.; Robinson, M.S. Lead in urban street dust. *Nature* **1975**, *253*, 343–345. [[CrossRef](#)]
4. Dreelin, E.A.; Fowler, L.; Carroll, C.R. A test of porous pavement effectiveness on clay soils during natural storm events. *Water Res.* **2006**, *40*, 799–805. [[CrossRef](#)] [[PubMed](#)]
5. Li, Y.; Helmreich, B. Simultaneous removal of organic and inorganic pollutants from synthetic road runoff using a combination of activated carbon and activated lignite. *Sep. Purif. Technol.* **2014**, *122*, 6–11. [[CrossRef](#)]
6. Müller, A.; Österlund, H.; Marsalek, J.; Viklander, M. The pollution conveyed by urban runoff: A review of sources. *Sci. Total Environ.* **2020**, *709*, 136125. [[CrossRef](#)]
7. Stokstad, E. Why were salmon dying? The answer washed off the road. *Science* **2020**, *370*, 1145. [[CrossRef](#)]
8. Sharma, V.K.; Fortuna, F.; Mincarini, M.; Berillo, M.; Cornacchia, G. Disposal of waste tyres for energy recovery and safe environment. *Appl. Energy* **2000**, *65*, 381–394. [[CrossRef](#)]
9. Xu, X.; Leng, Z.; Lan, J.; Wang, W.; Yu, J.; Bai, Y.; Sreeram, A.; Hu, J. Sustainable practice in pavement engineering through value-added collective recycling of waste plastic and waste tyre rubber. *Engineering* **2021**, *7*, 857–867.
10. Hong, N.; Guan, Y.; Yang, B.; Zhong, J.; Zhu, P.; Ok, Y.S.; Hou, D.; Tsang, D.C.W.; Guan, Y.; Liu, A. Quantitative source tracking of heavy metals contained in urban road deposited sediments. *J. Hazard. Mater.* **2020**, *393*, 122362. [[CrossRef](#)]
11. Tian, Z.; Zhao, H.; Peter, K.T.; Gonzalez, M.; Wetzel, J.; Wu, C.; Hu, X.; Prat, J.; Mudrock, E.; Hettinger, T.; et al. A ubiquitous tire rubber-derived chemical induces acute mortality in coho salmon. *Science* **2021**, *371*, 185–189. [[CrossRef](#)] [[PubMed](#)]
12. Fan, Z.; Lin, J.; Chen, Z.; Liu, P.; Wang, D.; Oeser, M. Multiscale understanding of interfacial behavior between bitumen and aggregate: From the aggregate mineralogical genome aspect. *Constr. Build. Mater.* **2021**, *271*, 121607. [[CrossRef](#)]
13. Viana, L.N.; Saint-Pierre, T.D. Direct determination of Cr and Ni in oil samples by isotope dilution and external standard calibration using inductively coupled plasma mass spectrometry. *Microchem. J.* **2019**, *151*, 104219. [[CrossRef](#)]
14. de Souza, V.S.; Sena Gomes Teixeira, L.; Sthefane, J.; Lima, S.O.; Ferreira da Mata Cerqueira, U.M.; Cordeiro de Oliveira, O.M.; de Souza Queiroz, A.F.; Almeida Bezerra, M. Analytical strategies for spectrometric determination of vanadium in samples of interest in the petroleum industry. *Appl. Spectrosc. Rev.* **2020**, *55*, 128–157. [[CrossRef](#)]
15. Sugiyama, I.; Williams-Jones, A.E. An approach to determining nickel, vanadium and other metal concentrations in crude oil. *Anal. Chim. Acta* **2018**, *1002*, 18–25. [[CrossRef](#)] [[PubMed](#)]
16. Gab-Allah, M.A.; Goda, E.S.; Shehata, A.B.; Gamal, H. Critical review on the analytical methods for the determination of sulfur and trace elements in crude oil. *Crit. Rev. Anal. Chem.* **2020**, *50*, 161–178. [[CrossRef](#)]
17. Niles, S.F.; Chacón-Patiño, M.L.; Putnam, S.P.; Rodgers, R.P.; Marshall, A.G. Characterization of an Asphalt Binder and Photo-products by Fourier Transform Ion Cyclotron Resonance Mass Spectrometry Reveals Abundant Water-Soluble Hydrocarbons. *Environ. Sci. Technol.* **2020**, *54*, 8830–8836. [[CrossRef](#)]
18. Brandt, H.C.A.; De Groot, P.C. Aqueous leaching of polycyclic aromatic hydrocarbons from bitumen and asphalt. *Water Res.* **2001**, *35*, 4200–4207. [[CrossRef](#)]
19. Abd El-Wahab, H.; Abd El-Fattah, M.; Gabr, M.Y. Preparation and characterization of flame retardant solvent base and emulsion paints. *Prog. Org. Coat.* **2010**, *69*, 272–277. [[CrossRef](#)]
20. Jin, X.Z.; Zheng, S.Z.; Li, R.Z.; Qiu, Y.; Cai, Y.P. Determination of soluble heavy metal Pb, Cd and Cr in water based architectural coatings for indoor decorating and refurbishing materials by ICP-AES. *Guang Pu Xue Yu Guang Pu Fen Xi Guang Pu* **2004**, *24*, 1127–1129.
21. Pan, Y.; Ye, Y.; CAI, J.; Yuan, J.; Liang, S.; Chen, Z. Determination of 18 Polycyclic Aromatic Hydrocarbons Migrated from Asphalt Based Waterproof Coating by Solid Phase Microextraction/Gas Chromatography-Mass Spectrometry. *J. Instrum. Anal.* **2018**, *37*, 772–777.
22. Li, T.; Lu, G.; Wang, D.; Oeser, M. Key Properties of High-performance Polyurethane Bounded Pervious Mixture. *China J. Highw. Transp.* **2019**, *32*, 158–169.
23. Lu, G.; Törzs, T.; Liu, P.; Zhang, Z.; Wang, D.; Oeser, M.; Grabe, J. Dynamic response of fully permeable pavement: The development of pore pressures subjected to different modes of loading. *ASCE's J. Mater. Civ. Eng.* **2020**, *32*, 04020160. [[CrossRef](#)]
24. Lu, G.; Wang, Z.; Liu, P.; Wang, D.; Oeser, M. The Investigation on the Hydraulic Properties of Pervious Pavement Mixtures: Characterization of Darcy and Non-Darcy Flow Based on Pore Microstructures. *ASCE's J. Transp. Eng. Part B Pavements* **2020**, *146*, 04020012. [[CrossRef](#)]
25. Chen, X.H.; Steinauer, B.; Wang, D.W. Evolution of aggregate surface texture due to tyre-polishing. *J. Cent. South Univ. Technol.* **2011**, *18*, 259–265. [[CrossRef](#)]
26. Wang, D.; Liu, P.; Wang, H.; Ueckermann, A.; Oeser, M. Modeling and testing of road surface aggregate wearing behaviour. *Constr. Build. Mater.* **2017**, *131*, 129–137. [[CrossRef](#)]
27. Wang, D.; Liu, P.; Oeser, M.; Stanjek, H.; Kollmann, J. Multi-scale study of the polishing behaviour of quartz and feldspar on road surfacing aggregate. *Int. J. Pavement Eng.* **2019**, *20*, 79–88. [[CrossRef](#)]

28. ASTM. ASTM D3319-2006 *Standard Practice for the Accelerated Polishing of Aggregate Using the British Wheel*; ASTM: West Conshohocken, PA, USA, 2017.
29. Lu, G.; Wang, Y.; Li, H.; Wang, D.; Oeser, M. The environmental impact evaluation on the application of permeable pavement based on life cycle analysis. *Int. J. Transp. Sci. Technol.* **2019**, *8*, 351–357. [[CrossRef](#)]
30. Lu, G.; Wang, H.; Zhang, Y.; Liu, P.; Wang, D.; Oeser, M.; Grabe, J. The hydro-mechanical interaction in novel polyurethane-bound pervious pavement by considering the saturation states in unbound granular base course. *Int. J. Pavement Eng.* **2021**, 1–14. [[CrossRef](#)]
31. Hong, B.; Lu, G.; Gao, J.; Wang, D. Evaluation of polyurethane dense graded concrete prepared using the vacuum assisted resin transfer molding technology. *Constr. Build. Mater.* **2021**, *269*, 121340. [[CrossRef](#)]
32. Trujillo-González, J.M.; Torres-Mora, M.A.; Keesstra, S.; Brevik, E.C.; Jiménez-Ballesta, R. Heavy metal accumulation related to population density in road dust samples taken from urban sites under different land uses. *Sci. Total Environ.* **2016**, *553*, 636–642. [[CrossRef](#)]
33. Yesilkanat, C.M.; Kobya, Y. Spatial characteristics of ecological and health risks of toxic heavy metal pollution from road dust in the Black Sea coast of Turkey. *Geoderma Reg.* **2021**, *25*, e00388. [[CrossRef](#)]
34. Heidari, M.; Darijani, T.; Alipour, V. Heavy metal pollution of road dust in a city and its highly polluted suburb; quantitative source apportionment and source-specific ecological and health risk assessment. *Chemosphere* **2021**, *273*, 129656. [[CrossRef](#)]
35. Wahab, M.I.A.; Abd Razak, W.M.A.; Sahani, M.; Khan, M.F. Characteristics and health effect of heavy metals on non-exhaust road dusts in Kuala Lumpur. *Sci. Total Environ.* **2020**, *703*, 135535. [[CrossRef](#)]
36. Apeagyei, E.; Bank, M.S.; Spengler, J.D. Distribution of heavy metals in road dust along an urban-rural gradient in Massachusetts. *Atmos. Environ.* **2011**, *45*, 2310–2323. [[CrossRef](#)]
37. Men, C.; Wang, Y.; Liu, R.; Wang, Q.; Miao, Y.; Jiao, L.; Shoaib, M.; Shen, Z. Temporal variations of levels and sources of health risk associated with heavy metals in road dust in Beijing from May 2016 to April 2018. *Chemosphere* **2021**, *270*, 129434. [[CrossRef](#)] [[PubMed](#)]
38. Pan, H.; Lu, X.; Lei, K. A comprehensive analysis of heavy metals in urban road dust of Xi'an, China: Contamination, source apportionment and spatial distribution. *Sci. Total Environ.* **2017**, *609*, 1361–1369. [[CrossRef](#)]
39. Zhao, L.; Hu, G.; Yan, Y.; Yu, R.; Cui, J.; Wang, X.; Yan, Y. Source apportionment of heavy metals in urban road dust in a continental city of eastern China: Using Pb and Sr isotopes combined with multivariate statistical analysis. *Atmos. Environ.* **2019**, *201*, 201–211. [[CrossRef](#)]
40. Adila, H.; Mamattursun, E.; Gulbanu, H.; Jin, W.; Anwar, M.; Alimujiang, K. Pollution and health risks assessment of heavy metals of road dust in Korla City, Xinjiang. *Geol. China* **2020**, *47*, 1915–1925.
41. Huang, B.; Zhou, Y.; Chang, W.; Li, Z.; Zeng, H. Differential Characteristics of Heavy Metal Pollution in Road Dust and Its Ecological Risk in Different Function Areas of Shenzhen City. *Ecol. Environ. Sci.* **2020**, *47*, 1915–1925.